Distributed Beat Length Measurement in Single-Mode Optical Fibers Using Stimulated Brillouin-Scattering and Frequency-Domain Analysis

Torsten Gogolla and Katerina Krebber

***Abstract*—We present a method for distributed measurement of beat length, differential group delay, strain, and temperature in long length single-mode optical fibers. Toward this aim, we employ the polarization state sensitive effect of stimulated Brillouin scattering (SBS). The distributed measurement is realized by applying frequency-domain analysis. We present the analytical relationships between the Brillouin interaction of two counterpropagating waves in the fiber and the polarization states. Experimental results confirm the ability of the method to measure distributed beat length.**

***Index Terms*—Beat length, differential group delay, distributed measurement, optical-fiber frequency-domain analysis, polarization mode dispersion, single-mode fibers (SMF's), stimulated Brillouin scattering (SBS).**

I. Introduction

OPTICAL fibers have become important elements in communication network systems due to their high efficiency of light transport and their large bandwidth. Single-mode fibers (SMF's) imply the highest bandwidth because of their low dispersion. However, in practice these fibers are two-mode fibers, because orthogonal components of the electrical field strength of the light guided in the fiber have different propagation constants due to birefringence. This birefringence is caused by internal and external stress and by non perfect circularity of the fiber core. If the chromatic dispersion is small, the birefringence induced polarization mode dispersion (PMD), i.e., the differential group delay (DGD) between two polarization modes, will be the most dominant effect that reduces the transmission capacity of single-mode fibers. Since the signal-to-noise ratio (SNR) in broadband digital and analog fiber-optic transmission systems is reduced as well [1]–[3] by the described effect, the knowledge of DGD is of high interest. Various methods have been used for the PMD measurement [4]–[8]. However, these methods give no distributed information about DGD along the fiber but only the overall DGD of the link. Further, they are quite expensive. A method for distributed measurement is proposed by [9]. They use the optical time-domain reflectometry (OTDR), where a short laser pulse is sent along the fiber and the backscattered Rayleigh light is detected with high temporal resolution. For the measurement of DGD, the polarization state of the backscattered Rayleigh light is evaluated.

In this paper, we present a measurement method based on the stimulated Brillouin interaction of two counterpropagating waves in the fiber [25]. The use of Brillouin scattering for distributed fiber measurements was demonstrated by Horiguchi and Tateda in 1989 [10]. They used a counterpropagating pulsed pump wave and a cw Stokes probe wave and estimated the fiber loss from the Brillouin amplification of the Stokes wave. A first theoretical investigation of this method, named Brillouin optical-fiber time-domain analysis (BOTDA), was also carried out by Horiguchi and Tateda [11]. Because of the temperature and strain dependence of the frequency shift between the pump and the Stokes waves, so called Brillouin frequency shift, BOTDA sensor systems can be used not only for fiber attenuation measurement but also for distributed temperature and strain measurement [12]–[15]. The sensing methods mentioned above all work in the time domain, which means the spatial resolution is realized by sending a short pulse along the fiber and detecting the transmitted or backscattered light with high temporal resolution. An alternative approach for distributed measurement is the frequency-domain method, which determines the transfer function of a length of fiber. Optical frequency-domain reflectometry (OFDR) is analyzed in detail, e.g., by Ghafoori-Shiraz and Okoshi [16]. The Brillouin optical-fiber frequency-domain analysis (BOFDA) is the frequency-domain alternative to the well-known BOTDA sensor concept for distributed temperature and strain measurement. This technique has been analyzed by [17]–[20]. Since the Brillouin interaction strength is additionally sensitive to the evaluation of polarization states of the pump and Stokes waves in the fiber, the Brillouin effect can be used for the measurement of DGD as well. Hence, this paper describes a completely new technique for distributed measurement of DGD based on the BOFDA sensor scheme.

In Section II, we describe the stimulated Brillouin effect and present a theoretical analysis of the polarization state dependence of the fiber-optic Brillouin interaction. Section III is involved with the distributed measurement, where the BOFDA system is employed. Section IV shows a method, with which the distributed DGD can be calculated from the BOFDA sensor signal. Section V, finally, presents some experimental results.

Manuscript received November 5, 1999; revised February 12, 1999. This work was supported by the "Ministerium für Wissenschaft und Forschung des Landes NRW" (Germany), Bennigsen-Foerder-Award 1997.

T. Gogolla is with the Business Unit Positioning, Hilti AG, Schaan FL-9494, Principality of Liechtenstein.

K. Krebber is with the Institute AEEO, Ruhr-University, Bochum D-44780, Germany.

Publisher Item Identifier S 0733-8724(00)02195-2.

II. Polarization State Dependence of Stimulated Brillouin Interaction

Fig. 1 shows the waves involved with the stimulated Brillouin interaction. Here, the narrow width pump light of field strength $E_P(0)$ is coupled into the near end of the fiber at $z = 0$ and the narrow width probe light of field strength $E_R(L)$ is coupled into the far end at $z = L$. Thus, the probe wave at $z = L$ is the boundary condition $E_S(L)$ of the Stokes wave in the fiber. The frequency of the probe light f_S is downshifted compared to that of the pump light f_P. If the frequency difference $f_D = f_P - f_S$ equals the characteristic Brillouin frequency f_B of the fiber, the acoustic wave ρ will be excited. Consequently, a maximum Brillouin interaction between the pump, Stokes, and acoustic waves occurs and a power conversion between the counterpropagating pump and Stokes waves takes place. Therefore, the Stokes wave $E_S(z)$ is damped by the fiber attenuation and simultaneously it experiences Brillouin gain while it travels along the fiber.

The fiber-optic Brillouin interaction with $f_D = f_B$ can be described by three partial differential equations:

$$\left[\frac{\partial}{\partial t} + \frac{c}{n}\frac{\partial}{\partial z} + \frac{c}{n}\alpha\right]\underline{\vec{E}}_P = j\frac{n^2 p_{12}\pi c}{\lambda\rho_0}\rho\underline{\vec{E}}_S \tag{1a}$$

$$\left[\frac{\partial}{\partial t} - \frac{c}{n}\frac{\partial}{\partial z} + \frac{c}{n}\alpha\right]\underline{\vec{E}}_S = j\frac{n^2 p_{12}\pi c}{\lambda\rho_0}\rho^*\underline{\vec{E}}_P \tag{1b}$$

$$\left[\frac{\partial}{\partial t} + c_S\frac{\partial}{\partial z} + \gamma_S\right]\rho = j\frac{\varepsilon_0 n^5 p_{12}\pi}{2\lambda c_S}\underline{\vec{E}}_P\underline{\vec{E}}_S^* \tag{1c}$$

where t is the time, z the fiber location, c the speed of light in vacuum, c_S the speed of the acoustic wave, n the refractive index of the fiber core, α the fiber attenuation coefficient of the field strength, γ_S the attenuation coefficient of the acoustic wave, p_{12} the elasto-optic coefficient of the fiber material, λ the wavelength of the pump light, ρ_0 the average density of the fiber material, and ε_0 the influence constant of vacuum. $\underline{\vec{E}}_P$, $\underline{\vec{E}}_S$, and ρ are complex amplitudes of the pump, Stokes, and acoustic waves in the fiber. They are dependent on z and t. Since the difference between the pump and Stokes wavelengths is very small, the relation $\lambda \cong \lambda_S \cong \lambda_P$ is used in (1a)–(c). Now, we assume a fiber length L of homogenous birefringence and polarized harmonic waves in form of

$$\vec{E}_P = \hat{E}_P(t,z) \times \begin{pmatrix} \cos(\alpha_P)\cos(2\pi f_P t + \varphi_P(t,z) - k_{P,x}z + \delta_P) \\ \sin(\alpha_P)\cos(2\pi f_P t + \varphi_P(t,z) - k_{P,y}z - \delta_P) \end{pmatrix} \tag{2a}$$

and

$$\vec{E}_S = \hat{E}_S(t,z) \times \begin{pmatrix} \cos(\alpha_S)\cos(2\pi f_S t + \varphi_S(t,z) - k_{S,x}(L-z) + \delta_S) \\ \sin(\alpha_S)\cos(2\pi f_S t + \varphi_S(t,z) - k_{S,y}(L-z) - \delta_S) \end{pmatrix} \tag{2b}$$

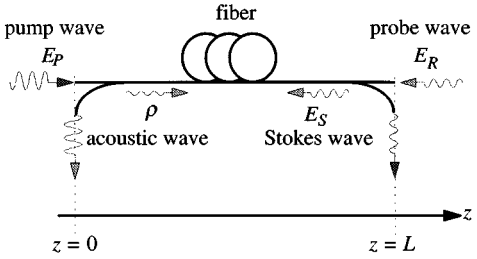

Fig. 1. Waves involved with stimulated Brillouin interaction.

with the complex amplitudes

$$\begin{aligned}\underline{\vec{E}}_P &= \underline{\hat{E}}_P(t,z)\begin{pmatrix} \cos(\alpha_P)\exp(-jk_{P,x}z + j\delta_P) \\ \sin(\alpha_P)\exp(-jk_{P,y}z - j\delta_P)\end{pmatrix} \\ &= \underline{\hat{E}}_P(t,z)\exp(-jk_{P,0}z) \\ &\quad\times\begin{pmatrix} \cos(\alpha_P)\exp(-j0.5\Delta k_P z + j\delta_P) \\ \sin(\alpha_P)\exp(+j0.5\Delta k_P z - j\delta_P)\end{pmatrix}\end{aligned} \tag{2c}$$

$$\begin{aligned}\underline{\vec{E}}_S &= \underline{\hat{E}}_S(t,z)\begin{pmatrix} \cos(\alpha_S)\exp(jk_{S,x}(z-L) + j\delta_S) \\ \sin(\alpha_S)\exp(jk_{S,y}(z-L) - j\delta_S)\end{pmatrix} \\ &= \underline{\hat{E}}_S(t,z)\exp(jk_{S,0}(z-L)) \\ &\quad\times\begin{pmatrix} \cos(\alpha_S)\exp(j0.5\Delta k_S(z-L) + j\delta_S) \\ \sin(\alpha_S)\exp(-j0.5\Delta k_S(z-L) - j\delta_S)\end{pmatrix}\end{aligned} \tag{2d}$$

$$\underline{\hat{E}}_P(t,z) = \hat{E}_P(t,z)\exp(j\varphi_P(t,z)) \tag{2e}$$

and

$$\underline{\hat{E}}_S(t,z) = \hat{E}_S(t,z)\exp(j\varphi_S(t,z)). \tag{2f}$$

α_S and α_P are the initial angles of the entered pump and Stokes field strength vectors with respect to the slow and fast axes of propagation (x- and y-components of field strengths). δ_S and δ_P describe the initial states of polarization of the waves fed into both ends of the fiber. If δ_S and δ_P are 0 or $\pi/2$, the entered waves will be linear polarized. If they are $\pi/4$, they will be circular polarized. Other values for δ_S and δ_P characterize elliptical polarization states. The phase terms φ_S and φ_P are insignificant for this consideration and consequently they will not be closer described. $k_{P,x}$ and $k_{P,y}$ are wave numbers of the x- and y-components of the pump wave field strength and $k_{S,x}$ and $k_{S,y}$ are that of the Stokes wave. The wave numbers for the Stokes and pump waves are slightly different, because the Stokes frequency is downshifted compared to that of the pump one. The wave numbers of the x- and y-components of the field strengths are different because of fiber birefringence. Further, it is

$$\Delta k_P = k_{P,x} - k_{P,y} = \frac{2\pi f_P}{c}(n_x - n_y) \tag{2g}$$

$$\Delta k_S = k_{S,x} - k_{S,y} = \frac{2\pi f_S}{c}(n_x - n_y) \tag{2h}$$

$$k_{P,x} = k_{P,0} + 0.5\Delta k_P \tag{2i}$$

$$k_{P,y} = k_{P,0} - 0.5\Delta k_P \tag{2j}$$

$$k_{S,x} = k_{S,0} + 0.5\Delta k_S \tag{2k}$$

and

$$k_{S,y} = k_{S,0} - 0.5\Delta k_S. \tag{2l}$$

n_x and n_y are the refractive index's of the x- and y-directions. Since the frequency dependence of the refractive index's is weak, it is neglected in this paper. Even for high birefringence fibers, the difference $n_x - n_y$ is very small. Therefore, in (1a)–(c) the relation $n \cong n_x \cong n_y$ can be used. The refractive index's must be distinguished only in the phase terms, where the difference $n_x - n_y$ exists. This can not be neglected.

The attenuation coefficient of the acoustic wave for typical single-mode fibers is about $\gamma_S = 1.6 \cdot 10^8$ s^{-1}. Consequently, for field strength variations which are finished in periods $t \gg \gamma_S^{-1} \approx 6,4$ ns, (1c) can be simplified

$$\gamma_S \rho = j\frac{\varepsilon_0 n^5 p_{12}\pi}{2\lambda c_S}\underline{\vec{E}}_P\underline{\vec{E}}_S^*. \tag{3a}$$

With (2c)–(d) and (3a), it follows:

$$\begin{aligned}\rho = j\frac{\varepsilon_0 n^5 p_{12}\pi \hat{\underline{E}}_P(t,z)\hat{\underline{E}}_S^*(t,z)}{\lambda\gamma_S c_S} \\ \times \exp[-j(k_{P,0}+k_{S,0})z + jk_{S,0}L] \\ \times [\cos(\alpha_S - \alpha_P)\cos(\Psi) - j\cos(\alpha_S+\alpha_P)\sin(\Psi)].\end{aligned} \tag{3b}$$

with

$$\Psi = 0.5(\Delta k_P + \Delta k_S)z - 0.5\Delta k_S L + \delta_S - \delta_P. \tag{3c}$$

For unstrained standard single-mode fibers at a temperature of 23 °C, the Stokes frequency f_S is about 12.8 GHz less than the pump one f_P, where $f_P = 227$ THz is assumed [18]. Consequently, the relative difference

$$\frac{\Delta k_P - \Delta k_S}{\Delta k_P} = \left(1 - \frac{f_S}{f_P}\right) < 6 \cdot 10^{-5} \tag{4}$$

is very small and the approximation $\Delta k_P \cong \Delta k_S \cong \Delta k$ is feasible. Multiplying (1a) with $\underline{\vec{E}}_P^*$, (1b) with $\underline{E}_S^*$, and using the relations

$$\frac{\partial(\underline{\vec{E}}_P\underline{\vec{E}}_P^*)}{\partial u} = \frac{\partial\underline{\vec{E}}_P}{\partial u}\underline{\vec{E}}_P^* + \frac{\partial\underline{\vec{E}}_P^*}{\partial u}\underline{\vec{E}}_P$$

and

$$\frac{\partial(\underline{\vec{E}}_S\underline{\vec{E}}_S^*)}{\partial u} = \frac{\partial\underline{\vec{E}}_S}{\partial u}\underline{\vec{E}}_S^* + \frac{\partial\underline{\vec{E}}_S^*}{\partial u}\underline{\vec{E}}_S$$

$(u = z, t)$, one obtains form (3b) and (1a)–(b)

$$\left[\frac{n}{c}\frac{\partial}{\partial t} + \frac{\partial}{\partial z} + \alpha\right] I_P = -\gamma g_B I_P I_S \tag{5a}$$

$$\left[\frac{n}{c}\frac{\partial}{\partial t} - \frac{\partial}{\partial z} + \alpha\right] I_S = \gamma g_B I_P I_S \tag{5b}$$

with the polarization factor

$$\begin{aligned}\gamma = \frac{1}{2}[\cos^2(\alpha_S - \alpha_P) - \cos^2(\alpha_S + \alpha_P)] \\ \times [1 + \cos[2\Delta k \cdot z - \Delta k \cdot L + 2(\delta_S - \delta_P)]] \\ + \cos^2(\alpha_S + \alpha_P)\end{aligned} \tag{5c}$$

the intensity of the pump wave

$$I_P = \frac{n\varepsilon_0 c}{2}|\hat{\underline{E}}_P|^2 \tag{5d}$$

and the Stokes one

$$I_S = \frac{n\varepsilon_0 c}{2}|\hat{\underline{E}}_S|^2. \tag{5e}$$

The dependence of the Brillouin gain coefficient g_B on the frequency difference $f_D = f_P - f_S$ is of Lorentz shape [18]:

$$g_B = \frac{\hat{g}_B}{1 + 4\left(\frac{f_D - f_B}{\Delta f_B}\right)} \tag{6a}$$

where $\hat{g}_B$ is the maximum gain coefficient at zero detuning $(f_D = f_P - f_S = f_B)$ and Δf_B the bandwidth of the Brillouin gain profile. For standard SMF's, they are $\hat{g}_B = 2.26 \cdot 10^{-11}$ m/W and $\Delta f_B = 50$ MHz. The maximum Brillouin gain coefficient is given by

$$\hat{g}_B = \frac{2\pi^2 n^7 p_{12}^2}{c\lambda^2\rho_0\gamma_S c_S}. \tag{6b}$$

In order to initiate Brillouin interaction in the fiber, the pump and Stokes waves have to produce a propagating interference pattern, which excites an acoustic wave by electrostriction (see (1c)). By this acoustic wave Brillouin interaction between the pump and Stokes waves is induced (see (1a)–(b)). Interference occurs only for parallel field strengths components of the pump and Stokes waves. When the polarization factor γ is not equal to unity, the polarization states of the pump and Stokes waves are different and only that component of the Stokes field strength vector which is at a certain position in the fiber parallel to that of the pump wave experience Brillouin gain. In this case, the Brillouin gain coefficient is reduced by the polarization factor γ. However, the Brillouin gain for the orthogonal component of the Stokes field strength vector is zero. The apparent maximum Brillouin gain coefficient $\gamma\hat{g}_B$, which is influenced by the polarization states of the pump and Stokes waves, can be measured by a BOFDA or BOTDA at each fiber location z. Since the characteristic Brillouin frequency f_B depends linear on fiber strain and temperature [18], the maximum of (6a) has to be found at each fiber location z by varying the frequency difference f_D between the pump and probe lasers.

The beat length L_B is given by the distance between two fiber locations where the polarization states of a wave are identical. In this case, the phase difference between the x- and y-components of the field strength from (2a) is

$$k_{P,x}L_B - k_{P,y}L_B = 2\pi$$

and with (2i), (2j), and (4), it follows:

$$L_B = \frac{2\pi}{\Delta k} = \frac{c}{f_P|n_x - n_y|} = \frac{\lambda_P}{|n_x - n_y|} \cong \frac{c^2}{n^2 f_P \Delta c} \quad (7)$$

where Δc is the velocity difference between the orthogonal field strength components. By evaluating the measured maximum Brillouin gain coefficient $\gamma \hat{g}_B$ as a function of the fiber location z with respect to the complete spatial cycle L_P, one obtains from (5c) the relation $2\Delta k L_P = 2\pi$. Hence, with (7), it follows:

$$L_B = 2L_P. \quad (8)$$

The differential group delay per unit fiber length is, from elementary theory [24]

$$\frac{d\Delta\tau}{dz} = \frac{d\Delta k}{d\omega} = \frac{|n_x - n_y|}{c} + \frac{2\pi f_P}{c}\left|\frac{dn_x}{d\omega} - \frac{dn_y}{d\omega}\right|. \quad (9a)$$

$\Delta\tau$ is the total differential group delay of the fiber. In weakly guiding fibers of doped silica, the dispersion in the near-infrared is very weak, i.e.

$$\left|\frac{dn_x}{d\omega} - \frac{dn_y}{d\omega}\right| \ll \frac{|n_x - n_y|}{\omega}.$$

Therefore, the last term in (9a) can be neglected [24] and it remains

$$\Delta\tau' = \frac{d\Delta\tau}{dz} \cong \frac{|n_x - n_y|}{c} \cong \frac{n^2}{c^2}\Delta c = \frac{1}{f_P L_B}. \quad (9b)$$

If Ψ from (3c) is zero and $\alpha_S - \alpha_P = \pi/2$, then the field strength vectors of the pump and Stokes waves are orthogonal and consequently the polarization factor γ will be zero and no Brillouin interaction exists at the fiber location z. In the case of $\alpha_P = 0$ or $\alpha_S = 0$, i.e., if the field strength vector of the pump or Stokes waves is oriented along the slow or fast axis of the fiber, then the first term in (5c) is zero and consequently, the spatial cycle L_P cannot be determined. In order to prevent this state, the orientation of the entered field strength must be changed by adjusting the polarization before coupling the waves into the fiber ends. Further, the axes of birefringence, i.e., the fast and slow axes can alter abruptly along the z-axis of the fiber. Here, fiber lengths of a spatial constant axis of birefringence are called rotation lengths [9]. In the following investigation, the fiber is composed of various fiber sections of homogenous beat and rotation lengths. Different axes of birefringence of the composed fiber cause different initial orientations α_S and α_P of the Stokes and pump field strengths at the opposite ends of the fiber sections. Consequently, the angles α_S and α_P and the amplitude of the polarization factor γ can change abruptly and randomly from one fiber section to another. If $\alpha_P \neq 0$ and $\alpha_S \neq 0$, in a section of spatially constant rotation length, the polarization factor γ is periodic and the complete spatial cycle L_P and thus the beat length L_B can be determined by the following BOFDA method for distributed measurements. For the few fiber sections where $\alpha_P = 0$ or $\alpha_S = 0$, the initial orientation of the entered field strength vectors must be changed and then the measurement must be repeated.

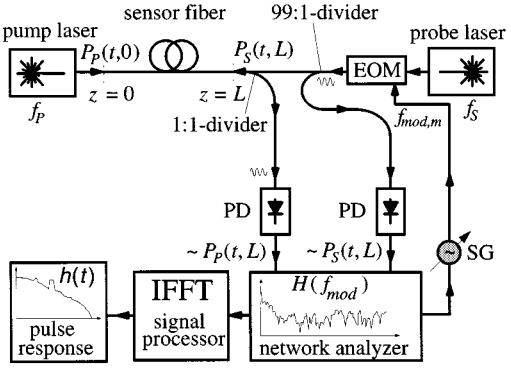

Fig. 2. Basic configuration of a BOFDA.

III. The Brillouin Optical Frequency Domain Analysis

The Brillouin optical frequency-domain analysis is based on the measurement of a complex baseband transfer function that relates the complex amplitudes of counterpropagating pump and Stokes powers at one end of a fiber [17]–[19]. One experimental configuration of a BOFDA sensor system is shown in Fig. 2. The cw light of a narrow-linewidth pump laser is coupled into one end of a single-mode fiber. At the other end the cw light of a narrow-linewidth probe laser is coupled in, whose frequency is downshifted by the difference $f_{D,0}$ compared with that of the pump laser. Here, the probe-induced Brillouin loss of the pump wave is used.

The light of the probe laser is modulated in amplitude by an electrooptic modulator (EOM) with a variable modulation frequency $f_{\mathrm{mod},m}$. The modulated intensity of the probe laser is the boundary condition for the Stokes wave that interacts with the pump wave in the fiber. Consequently, the initial constant pump power obtains an alternating part as well. For each value of $f_{\mathrm{mod},m}$, the modulated probe power that equals the Stokes power $P_S(t,L)$ at $z = L$ and the alternating part of the transmitted modulated pump power $P_P(t,L)$ are recorded. The output signals of the photodetectors (PD's), which are proportional to the modulated pump and Stokes powers at $z = L$, are fed to a network analyzer (NWA). Here, the signals are down-converted to a low-frequency range, digitized by analog-to-digital converter, and fed to a digital signal processor which calculates and stores the phase and amplitude data of the down-converted signals. These measured amplitude and phase information agree with those of the detected optical powers at the adjusted modulation frequency. Hereafter, the frequency is increased and the same procedure is executed. Thus, the amplitudes and phases of the detected Stokes and pump powers are successively measured by the network analyzer at M equidistant modulation frequencies $f_{\mathrm{mod},m} = m\Delta f_{\mathrm{mod}}$, with $m = 0, 1, 2, \ldots, M-1$. Δf_{mod} is the frequency step. The modulated probe power at $z = L$ can be described as

$$P_S(t,L) = \bar{P}_{S,L} + \hat{P}_{S,L}(f_{\mathrm{mod},m}) \times \cos(2\pi f_{\mathrm{mod},m} t + \Phi_{S,L}(f_{\mathrm{mod},m})) \quad (10)$$

where $\bar{P}_{S,L}$ is the average value, $\hat{P}_{S,L}(f_{\mathrm{mod},m})$ the amplitude, and $\Phi_{S,L}(f_{\mathrm{mod},m})$ the initial phase. The amplitude and phase are weakly dependent on $f_{\mathrm{mod},m}$. The transmitted pump power

at $z = L$, which is influenced by the modulated Stokes power in the fiber, is given by

$$P_P(t, L) = \bar{P}_{P,L} + \hat{P}_{P,L}(f_{\mathrm{mod},m}) \times \cos(2\pi f_{\mathrm{mod},m} t + \Phi_{P,L}(f_{\mathrm{mod},m})) \quad (11)$$

where $\bar{P}_{P,L}$ is the average value of the transmitted pump power. Here, the amplitude $\hat{P}_{P,L}(f_{\mathrm{mod},m})$ and phase $\Phi_{P,L}(f_{\mathrm{mod},m})$ are influenced by temperature, strain, polarization state distribution, and fiber attenuation. They are strongly dependent on the modulation frequency. With the stored amplitude and phase values, the digital signal processor determines the discrete, complex modulation transfer function:

$$H(f_{\mathrm{mod},m}) = \frac{\hat{P}_{P,L}(f_{\mathrm{mod},m})}{\hat{P}_{S,L}(f_{\mathrm{mod},m})} \exp\{j\Phi_{P,L}(f_{\mathrm{mod},m}) - j\Phi_{S,L}(f_{\mathrm{mod},m})\} \quad (12)$$

Subsequently, the signal processor calculates the invers fast Fourier transform (IFFT) of this discrete transfer function. For a linear system, this IFFT is a good approximation of the discrete pulse response according to the Brillouin interaction at the adjusted frequency difference $f_{D,0}$ between pump and probe lasers. It is

$$h(t_q, f_{D,0}) = \mathbf{IFFT}\{H(f_{\mathrm{mod},m})\} \quad (13)$$

where $t_q = q\Delta t$, with $q = 0, 1, 2, \ldots, M-1$. Δt is the temporal resolution. The sensor signal is finally given by the real part of the pulse response:

$$h_{\mathrm{sens}}(z_q, f_{D,0}) = \mathrm{Re}\{h(2z_q n_{\mathrm{gr}}/c, f_{D,0})\}. \quad (14)$$

In (14) the time coordinate t_q is substituted by $2z_q n_{\mathrm{gr}}/c$ in order to obtain a spatial resolution; n_{gr} denotes the group refractive index of the fiber core. It is $z_q = q\Delta z$ with the two-point resolution $\Delta z = \Delta t c/(2n_{\mathrm{gr}})$.

The physical pulse response $h_{\mathrm{ph}}(t)$, which is measured directly in the time domain, is real. The modulation transfer function $H_{\mathrm{ph}}(f_{\mathrm{mod}})$ is the Fourier transform of the real pulse response $h_{\mathrm{ph}}(t)$. For real pulse responses, it is $H_{\mathrm{ph}}(-f_{\mathrm{mod}}) = H^*_{\mathrm{ph}}(f_{\mathrm{mod}})$ [21]. In the frequency-domain analysis, the modulation transfer function $H(f_{\mathrm{mod}})$ is measured in the positive frequency range $0 < f_{\mathrm{mod}} \leq f_{\mathrm{mod,max}}$, with the maximum modulation frequency $f_{\mathrm{mod,max}} = \Delta f_{\mathrm{mod}}(M-1)$. Hence, $H(f_{\mathrm{mod}}) = 0$ for $f_{\mathrm{mod}} < 0$. Pulse responses of transfer functions, which are zero for negative frequencies, are complex [21]. In our special case, the transfer function can be considered as an invers Fourier transform of an analytical signal [21] and the physical pulse response is then given by the real part of the analytical one $h(t)$. The imaginary part of $h(t)$ is the Hilbert transform of the real part. It contains no further information.

If the strain or the temperature distribution and consequently the characteristic Brillouin frequency of the fiber are not homogeneous, the frequency difference between pump and probe lasers has to be varied in order to find the maximum of the Brillouin gain coefficient at each fiber location z. The frequency differences are $f_{D,r} = f_{D,0} + r\Delta f_D$ with $r = 0, 1, 2, \ldots, R-1$, where R is the number of the equidistant laser frequency differences and Δf_D is their step. The apparent Brillouin gain coefficient γg_B can be calculated with the measured Brillouin sensor signal [see (14)] as a function of the fiber location and the frequency difference between pump and probe lasers [20]. The maximum of this coefficient at each fiber location is at a frequency difference that equals the characteristic Brillouin frequency, which is linearly dependent on strain and temperature. Consequently, with the Brillouin frequencies of each fiber location, the strain or temperature at these locations can be calculated. Since $\hat{g}_B$ is constant, the polarization factor γ according to (5c) can be determined with the maximum apparent gain coefficient $\gamma\hat{g}_B$ at each fiber location z_q. The beat length can be calculated with (8) by finding out the complete spatial cycle L_P of γ in different fiber regions. Here, (8) follows according to Section II from the Brillouin equations (1a)–(c).

The maximum fiber length, which can be investigated by the frequency-domain approach, is limited by the modulation frequency step Δf_{mod}. The maximum length is given by [18]

$$L_{\max} = \frac{c}{2n_{\mathrm{gr}}} \frac{1}{\Delta f_{\mathrm{mod}}}. \quad (15)$$

The two-point resolution of a BOFDA sensor, which is the minimum resolvable distance between two points along the fiber, is [18]

$$\Delta z = \frac{c}{2n_{\mathrm{gr}}} \frac{1}{f_{\mathrm{mod,max}}}. \quad (16)$$

For a 10-km-long fiber and a spatial resolution of 1.22 m, the maximum modulation frequency and the frequency step are 81.96 MHz and 10 kHz, respectively. For this configuration, 8196 single measurements at equidistant modulation frequencies are necessary. Here, the IFFT requires $M = 2^q$ with $q = 1, 2, 3, \ldots$ In a BOTDA system, the two-point resolution is proportional to the time difference between two time-domain sampling points. It is equivalent to the reciprocal of the maximum modulation frequency $1/f_{\mathrm{mod,max}}$ for a frequency-domain measurement.

IV. Statistical Calculation of Beat Length

In the case of the Brillouin optical frequency-domain method, the polarization factor $\gamma(z_q)$ can be determined at discrete fiber locations z_q. This factor describes the statistical properties of the beat length along the single-mode fiber. In long fibers there exist many different beat lengths in different fiber regions. The beat length is given by complete spatial cycles of $\gamma(z_q)$ (see (8)). Hence, it can be found out by discrete Fourier transform (DFT) of intervals of $\gamma(z_q)$, in which the beat length has to be measured. Thus, it is

$$\Gamma(\xi_u) = \mathbf{DFT}\{\gamma(z_q)\} \quad (17)$$

with $q = Q_1, Q_1+1, \ldots, Q_2-1, Q_2$. z_{Q1} and z_{Q2} describe the interval limits. $\xi_u = u/(z_{Q2} - z_{Q1})$ with $u = 0, 1, \ldots, U-1$ and $U = Q_2 - Q_1$ are spatial frequencies. The measured spatial cycle is $L_{P,u} = 1/\xi_u$ and consequently with (8), it follows:

$$L_{B,u} = \frac{2}{\xi_u} \quad (18)$$

which means, several beat length $L_{B,u}$ can exist in the interval $[z_{Q1}, z_{Q2}]$. With (9b), the differential group delay is given by

$$\Delta\tau'_u \cong \frac{\xi_u}{2f_P}. \tag{19}$$

Now, we define the normalized transformed polarization factor

$$\Gamma_N(\xi_u) = \frac{\Gamma(\xi_u)}{\sum_{u=0}^{U-1}\Gamma(\xi_u)} \tag{20a}$$

so that

$$\sum_{u=0}^{U-1}\Gamma_N(\xi_u) = 1. \tag{20b}$$

Thus, for the total differential group delay in the fiber interval $[z_{Q1}, z_{Q2}]$, one can write

$$\begin{aligned}\Delta\tau' &= \sum_{u=0}^{U-1}\Delta\tau'_u \cdot \Gamma_N(\xi_u) \\ &= \sum_{u=0}^{U-1}\frac{\xi_u}{2f_P}\cdot\Gamma_N(\xi_u)\end{aligned} \tag{21}$$

and the equivalent beat length in this interval is given by (9b)

$$\bar{L}_B = \frac{1}{f_P\Delta\tau'}. \tag{22}$$

For the dominant beat length $L_{B,\mathrm{dom}}$, $\Gamma(\xi_{\mathrm{dom}})$ is maximum. By determining the equivalent beat lengths of various intervals, a distributed measurement of $\bar{L}_B$ is feasible.

V. Experimental Results

In the experiment, we use the BOFDA configuration according to Fig. 2. The test fiber is a standard GeO_2 doped SiO_2 single-mode fiber for the telecommunication. The core diameter is 9 μm, the refractive index of the core is about 1.47, and the characteristic Brillouin frequency of the unstrained fiber at a temperature of 23°C is 12.8 GHz. The strain and temperature coefficients of the Brillouin frequency are 500 MHz/% and 1.2 MHz/K, respectively. The maximum Brillouin gain coefficient is $2.26 \cdot 10^{-11}$ m/W. In the range 0 m $\leq z \leq$ 9600 m the fiber is wound on a drum 150 mm in diameter and in the range 9600 m $\leq z \leq$ 11 000 m, it is wound on one with a diameter of 1200 mm. The pump and the probe lasers are frequency-tunable single-mode diode-pumped Nd:YAG-ring lasers with a vacuum wavelength of 1319 nm, a linewidth of less than 5 kHz, and output powers of 160 and 1 mW, respectively. Both lasers are optically isolated. The frequency of the probe laser is downshifted compared with that of the pump laser. Since the strain in our test fiber differs with 0.17%, the frequency shift is varied between 12.75 and 12.95 GHz in steps of 5 MHz. For stabilizing the laser frequency difference, the beat signal of the pump and the probe light is detected by a 40-GHz-photodetector and is downconverted by a low-noise-satellite-converter (LNC) with a local oscillation frequency of 11.45 GHz. Consequently, the resulting electric signal at the converter output is in a frequency range between 1.3–1.5 GHz. It is fed to a frequency counter. A computer acquires the measured frequency, determines the frequency shift, and stabilizes it by temperature and piezo electric control of the laser resonators. The pump laser power is attenuated down to 1 mW before it is coupled into the test fiber. The probe laser power at the probe input is 400 μW. The probe light is intensity modulated by the EOM successively between 100 Hz and 18.2 MHz in steps of 8.9 kHz. Thus, in a maximum fiber length of 11.3 km, a spatial resolution of 5.5 m can be achieved. The average optical powers of the transmitted pump and probe light as well as the input one are measured by power meters. As described above, the NWA determines the complex modulation transfer function at equidistant modulation frequencies. The real part of the calculated pulse response gives the sensor signal (see (14)). This is determined at equidistant frequency differences f_D between pump and probe lasers. With this sensor signal and the measured average powers at the fiber ends, the apparent Brillouin gain coefficient γg_B can be calculated as a function of the fiber location z and the frequency difference f_D [20]. At each position z, the gain coefficient as a function of f_D is of Lorentz shape (see. (6a)). The maximums of these different located Lorentz functions are at $f_D = f_B(z)$. Since the Brillouin frequency $f_B(z)$ at the location z is linear dependent on strain and temperature, these quantities can be determined by evaluating the maximum Brillouin gain coefficient at each fiber location z.

In Fig. 3, a plot of the measured Brillouin gain coefficient is shown. Light areas represent high values and dark areas represent low values. At $z = 4.5$ km, the Brillouin frequency is 12.885 GHz and thus the strain of this 50 m long region is 0.17%. In this measurement, the spatial resolution is 22 m and consequently the Brillouin gain fluctuation caused by polarization variation will be equalized if the complete spatial cycle L_P from (8) is less than 22 m.

Evaluating the maximums of the Brillouin spectra at each location z, the strain distribution $\varepsilon(z)$ along the fiber can be determined. It is shown in Fig. 4. Employing a polarization scrambler before either the pump or the probe wave is coupled into the fiber, the polarization effects can be eliminated and the strain or temperature measurement can be improved.

However, for beat length measurement, the polarization effects are essential and the polarization scrambler has to be deactivated. In this case, the maximum apparent Brillouin gain coefficient is determined at each fiber location z. It is demonstrated in Fig. 5.

Here, the spatial resolution is 5.5 m and thus the Brillouin gain fluctuation originated by polarization variation is not equalized. At $z = 9.6$ km, the spatial cycle becomes larger because the drum diameter changes at this position. Dividing this maximum gain coefficient by the maximum possible value $2.26 \cdot 10^{-11}$ m/W, one obtains the polarization factor $\gamma(z)$. Evaluating this factor for various fiber regions, as shown in Section IV, one obtains the distribution of the equivalent beat length in defined intervals along the fiber. In Fig. 6, the normalized Fourier transform of $\gamma(z)$ according to (20a) in the interval 6420 m $< z <$ 6840 m is shown. The dominant spatial frequency is 0.0216

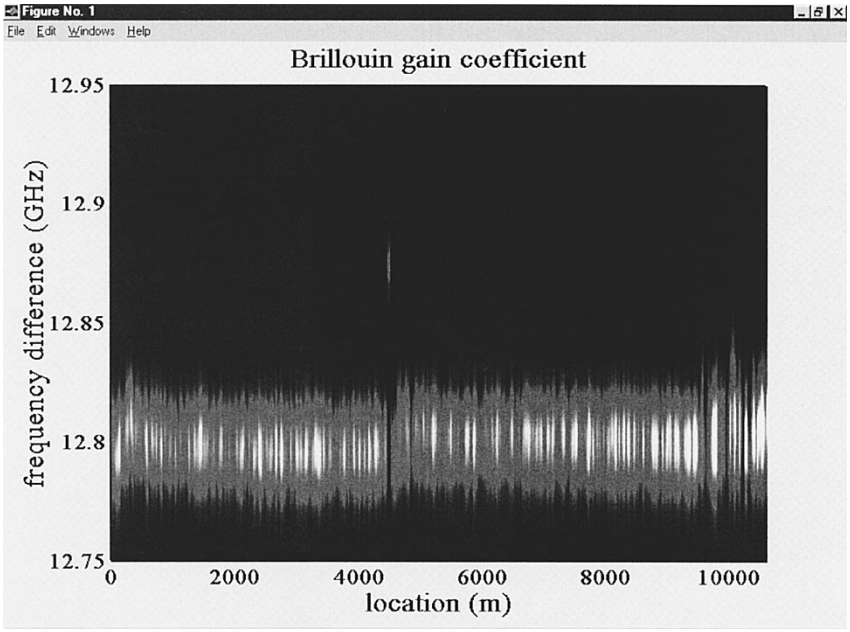

Fig. 3. Measured Brillouin gain coefficient as a function of fiber location z and frequency difference f_D.

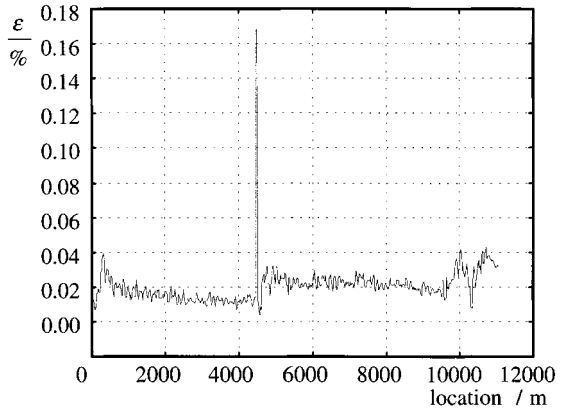

Fig. 4. Strain distribution $\varepsilon(z)$ along the fiber.

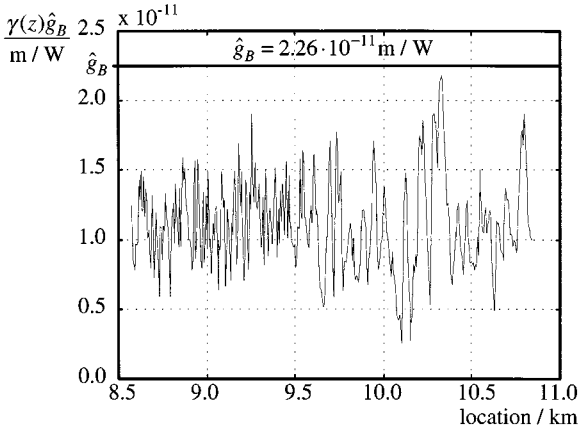

Fig. 5. Maximum apparent Brillouin gain coefficient as a function of fiber location.

m^{-1}. According to (18), the dominant beat length is 93 m and the equivalent one, which is calculated by (22), amounts to 58 m.

Fig. 7 illustrates the calculated beat length as a function of the fiber location z. Here, the equivalent beat length has been calculated in the intervals [0 m, 420 m], [5.5 m, 425.5 m], [11 m, 431 m], etc. In the range $0\,\text{m} < z < 9.6$ km, the equivalent beat length is around 55 m and for $z > 9.6$ km, it amounts to about 105 m. Thus, the differential group delays are 0.08 ps/km and 0.044 ps/km, respectively.

This measurement agrees good with that in [9], where they wound a single-mode fiber on a drum 100 mm in diameter and used a wavelength of 1550 nm. Here, a beat length of 29 m has been measured. In the range up to 9.6 km, we wound the fiber on a drum 150 mm in diameter and applied a wavelength of 1320 nm. The beat length is proportional to the wavelength (see (7)) and for small drum diameters d, it is proportional to the square of d [22]. Since it is

$$55\ \text{m} \cdot \left(\frac{100\ \text{mm}}{150\ \text{mm}}\right)^2 \frac{1550\ \text{nm}}{1320\ \text{nm}} = 28.7\ \text{m}$$

the 55 m beat length measured with our technique matches very good the 29 m beat length shown in [9]. The polarization factor γ as a function of the location z in Fig. 5 looks random. This is caused by abrupt changes of the rotation lengths, which in turn cause abrupt changes of α_P and α_S and thus of the amplitude of γ [see (5c)]. However, in Fig. 5 one can see that a change of the beat length at $z = 9.6$ km causes a significant change of the periodic cycle. Furthermore, the results of these measurements match very well theoretical results of wound fibers [22] and the results of Galtarossa *et al.*[9].

The frequency-domain method offers some advantages compared with the time-domain one [18], [23]. An important aspect is the possibility of narrow-bandwidth operation in the case of BOFDA. For BOTDA, broad-band measurements are necessary to resolve pulse rising times of several nanoseconds, but in a frequency-domain measurement the baseband transfer function is determined pointwise for each modulation frequency, thus, only one frequency component is measured by a network analyzer with a narrow resolution bandwidth (e.g., 100 Hz) at

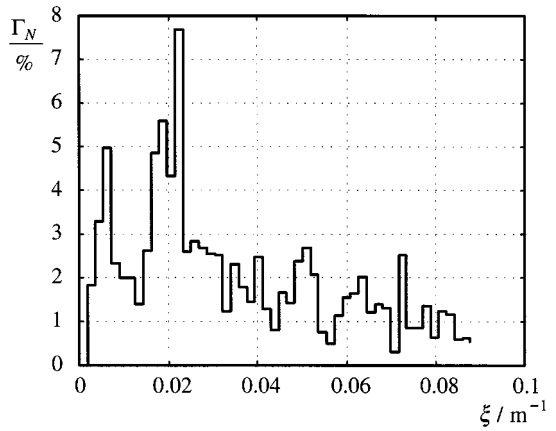

Fig. 6. Normalized Fourier transform Γ_N as a function of spatial frequency ξ.

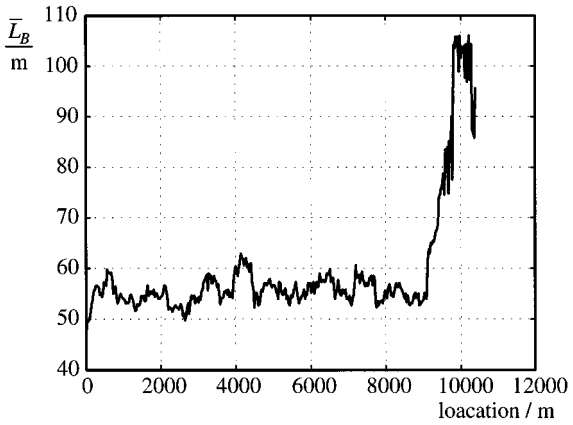

Fig. 7. Beat length as a function of the fiber location z.

each time. The resolution bandwidth is the bandwidth of the downconverted intermediate frequency signal, which contains the phase and amplitude of the detected signal. This IF-signal can be analyzed in a very narrow frequency band. Since the discrete Fourier transform induces additional averaging effects for uncorrelated noise signals, the noise level is far lower than that for a time-domain measurement [23]. However, in the time-domain, one applies high-power laser pulses which produce an adequate SNR, although the noise level is high. But in a BOFDA sensor, low-power grating stabilized diode lasers of wavelengths around 1300 or 1550 nm can be used. These wavelengths are essential for the telecommunication and thus for distributed beat length measurement.

VI. Conclusion

We present a method for distributed beat length measurement in optical SMF's based on stimulated Brillouin interaction of two counterpropagating laser waves. In order to realize a spatial resolution, we apply the Brillouin optical frequency-domain analysis (BOFDA), where sinusoidally intensity modulated laser light is evaluated with respect to amplitude differences and phase shifts at equidistant modulation frequencies. The dependence of the Brillouin gain coefficient on the polarization states of both waves in the fiber has been theoretically shown. Further, the BOFDA method has been presented and experimental results of a frequency-domain measurement demonstrate the feasibility of the BOFDA sensor concept for distributed strain, temperature, and beat length measurements. The results agree good with that of other methods.

References

[1] C. D. Poole, R. W. Tkach, A. R. Chraplyvy, and D. A. Fishman, "Fading in light wave systems due to polarization mode dispersion," *IEEE Photon. Technol. Lett.*, vol. 1, pp. 68–70, 1991.

[2] E. Iannone, F. Matera, A. Galtarossa, G. Gianello, and M. Schiano, "Effects of polarization dispersion on the performance of IM-DD communication systems," *IEEE Photon. Technol. Lett.*, vol. 10, pp. 1247–1249, 1993.

[3] C. D. Poole and T. E. Darcie, "Distortion related to polarization mode dispersion in analog lightwave systems," *J. Lightwave Technol.*, vol. 11, pp. 1749–1759, 1993.

[4] A. Galtarossa, G. Gianello, C. G. Someda, and M. Schiano, "In-field comparison among polarization-mode-dispersion measurement technique," *J. Lightwave Technol.*, vol. 14, pp. 42–49, 1996.

[5] B. L. Heffner, "Automated measurement of polarization mode dispersion using Jones matrix eigenanalysis," *IEEE Photon. Technol. Lett.*, vol. 4, pp. 1066–1069, 1992.

[6] F. Curti, B. Daino, G. De Marchis, and F. Matera, "Statistical treatment of the evolution of the principal states of polarization in single-mode fibers," *J. Lightwave Technol.*, vol. 8, pp. 1162–1166, 1990.

[7] C. D. Poole and D. L. Favin, "Polarization-mode dispersion measurement based on transmission spectra through a polarizer," *J. Lightwave Technol.*, vol. 12, pp. 917–929, 1994.

[8] N. Gisin, R. Passy, J. P. Von der Weid, and J. C. Bishoff, "Polarization-mode-dispersion measurements with all-fiber interferometer," in *Proc. OFC'94*, San Jose, CA, 1994, paper WK15, pp. 138–139.

[9] A. Galtarossa, F. Corsi, and L. Palmieri, "Experimental investigation of polarization mode dispersion properties in single-mode fibers using a new backscattering technique," in *Proc. Conf. Optic. Fiber Commun., Tech. Dig. Ser. 1998*. Piscataway, NJ, Feb. 1998, pp. 343–355.

[10] T. Horiguchi and M. Tateda, "Optical-fiber-attenuation investigation using stimulated Brillouin scattering between a pulse and a continuous wave," *Opt. Lett.*, vol. 14, no. 8, pp. 408–410, Apr. 1989.

[11] T. Horiguchi and M. Tateda, "BOTDA—Nondestructive measurement of single-mode optical fiber attenuation characteristics using Brillouin interaction: Theory," *J. Lightwave Technol.*, vol. 7, pp. 1170–1176, Aug. 1989.

[12] T. Kurashima, T. Horiguchi, and M. Tateda, "Distributed-temperature sensing using stimulated Brillouin scattering in optical silica fibers," *Opt. Lett.*, vol. 15, no. 8, pp. 1038–1040, Sept. 1990.

[13] X. Bao, J. Dhliwayo, N. Heron, D. J. Webb, and D. A. Jackson, "Experimental and theoretical studies on a distributed temperature sensor based on brillouin scattering," *J. Lightwave Technol.*, vol. 13, pp. 1340–1348, July 1995.

[14] X. Bao, D. J. Webb, and D. A. Jackson, "Combined distributed temperature and strain sensor based on Brillouin loss in an optical fiber," *Opt. Lett.*, vol. 19, no. 2, pp. 141–143, Jan. 1994.

[15] K. Shimizu, T. Horiguchi, and Y. Koyamada, "Measurement of distributed strain and temperature in a branched optical fiber network by use of Brillouin optical time-domain reflectometry," *Opt. Lett.*, vol. 20, no. 5, pp. 507–509, Mar. 1995.

[16] H. Ghafoori-Shiraz and T. Okoshi, "Fault location in optical fibers using optical frequency domain reflectrometry," *J. Ligthwave Technol.*, vol. LT-4, no. 3, pp. 316–322, 1986.

[17] D. Garus, T. Gogolla, K. Krebber, and F. Schliep, "Distributed sensing technique based on Brillouin optical-fiber frequency-domain analysis," *Opt. Lett.*, vol. 21, no. 17, pp. 1402–1404, Sept. 1996.

[18] D. Garus, T. Gogolla, K. Krebber, and F. Schliep, "Brillouin optical-fiber frequency-domain analysis for distributed temperature and strain measurements," *J. Lightwave Technol.*, vol. 15, pp. 654–662, Apr. 1997.

[19] T. Gogolla and K. Krebber, "Fiber sensors for distributed temperature and strain measurements using Brillouin scattering and frequency-domain methods," in *Proc. Conf. EnviroSense'97*, June 1997, pp. 168–179.

[20] E. Geinitz, S. Jetschke, U. Röpke, S. Schröter, and R. Willsch, "Improvement of distributed Brillouin sensing by compensation for systematic errors," in *Proc. Conf. OFS-11*, May 1997.

[21] A. Fettweis, *Elemente nachrichtentechnischer Systeme* Stuttgart, Germany, 1990.

[22] S. C. Rashleigh, "Origins and control of polarization effects in single-mode fibers," *J. Lightwave Technol.*, vol. LT-1, pp. 312–331, 1983.

[23] M. A. Farahani and T. Gogolla, "Spontaneous Raman scattering in optical fibers with modulated probe light for distributed temperature Raman remote sensing," *J. Lightwave Technol.*, vol. 17, pp. 1379–1391, Aug. 1999.
[24] S. C. Rashleigh and R. Ulrich, "Polarization mode dispersion in single-mode fibers," *Opt. Lett.*, vol. 3, no. 2, pp. 60–62, Aug. 1978.
[25] L. Thévenaz, "Evaluation of local birefringence along fibers using Brillouin analysis," in *Proc. OFMC'97*, Teddington, U.K., 1997, pp. 82–85.

Torsten Gogolla was born in Attendorn, Germany, in 1965. He received the diploma degree in electrical engineering from Ruhr-University of Bochum, Germany, in 1993. Between 1993 and 1999, he worked towards the Ph.D. degree at the Institute of Electrooptics at Ruhr-University.

His research interests include fiber-optic distributed sensing, nonlinear optics, laser radar techniques, and microwave applications. He is now with Hilti Corporation, Schaan, Principality of Liechtenstein.

Katerina Krebber was born in Plovdiv, Bulgaria, in 1963. She received the degree in physics from the University of Plovdiv in 1987. Since 1993, she has been working towards the Ph.D. degree with the Institute of Electrooptics at the Ruhr-University of Bochum, Germany.

From 1987 to 1989, she was engaged in research on optical fiber sensors in the Institute of Applied Physics in Plovdiv. Her research interests are in the field of nonlinear optics, optical fiber communication, and distributed fiber sensors.